



Pulse propagation in a 1D array of excitable semiconductor lasers

K. Alfaro-Bittner, Sylvain Barbay, M G Clerc

► To cite this version:

K. Alfaro-Bittner, Sylvain Barbay, M G Clerc. Pulse propagation in a 1D array of excitable semiconductor lasers. *Chaos: An Interdisciplinary Journal of Nonlinear Science*, 2020, 30 (8), <10.1063/5.0006195>. <hal-02865468>

HAL Id: hal-02865468

<https://hal.science/hal-02865468v1>

Submitted on 11 Jun 2020

HAL is a multi-disciplinary open access archive for the deposit and dissemination of scientific research documents, whether they are published or not. The documents may come from teaching and research institutions in France or abroad, or from public or private research centers.

L'archive ouverte pluridisciplinaire **HAL**, est destinée au dépôt et à la diffusion de documents scientifiques de niveau recherche, publiés ou non, émanant des établissements d'enseignement et de recherche français ou étrangers, des laboratoires publics ou privés.



HAL Authorization

Pulse propagation in a 1D array of excitable semiconductor lasers

K. Alfaro-Bittner,¹ S. Barbay,^{2, a)} and M.G. Clerc³

¹⁾ *Departamento de Física, Universidad Técnica Federico Santa María, Av. España 1680, Casilla 110V, Valparaíso, Chile.*

²⁾ *Centre de Nanosciences et de Nanotechnologies, CNRS, Université Paris-Saclay, 91120 Palaiseau, France.*

³⁾ *Departamento de Física and Millennium Institute for Research in Optics, FCFM, Universidad de Chile, Casilla 487-3, Santiago, Chile.*

Nonlinear pulse propagation is a major feature in continuously extended excitable systems. The persistence of this phenomenon in coupled excitable systems is expected. Here, we investigate theoretically the propagation of nonlinear pulses in a 1D array of evanescently coupled excitable semiconductor lasers. We show that the propagation of pulses is characterized by a hopping dynamics. The average pulse speed and bifurcation diagram are characterized as a function of the coupling strength between the lasers. Several instabilities are analyzed such as the onset and disappearance of pulse propagation, and a spontaneous breaking of the translation symmetry. The pulse propagation modes evidenced are specific to the discrete nature of the 1D array of excitable lasers.

Linear oscillators coupled with springs to nearest neighbors exhibit wave propagation. This phenomenon is persistent when considering the continuous limit, i.e. when considering an elastic rope. In this limit, the wave dispersion relation is linear, unlike the discrete case of coupled systems where it is nonlinear. Here we study the propagation of localized nonlinear waves—pulses—in coupled excitable systems. Excitable oscillators play a fundamental role in understanding the activity of neurons, cardiac tissue, and oscillatory chemical reactions. Based on a model of a 1D array of excitable semiconductor lasers, we show that pulse propagation is characterized by a hopping dynamics and that it displays a rich variety of bifurcations. Counterintuitively, we observe that pulses do not persist in the continuous limit.

I. INTRODUCTION

The propagation of excitations (spikes) in discrete excitable media plays a major role in biological systems^{1–4}. It is at the heart of the conduction of information in axons, and ensures conduction delays which are central to information processing in neural networks⁵. The possibility to process information with spikes in photonic systems has attracted recently a lot of interest because of its application potential in terms of energy consumption, parallelism and speed^{6–9}. It has been recently shown theoretically that coupled excitable semiconductor lasers can behave analogously to biological axons, allowing to transport and process information in the form of short optical spikes^{8,10}.

Dissipative systems are characterized by exhibiting attractors and basins of attraction^{11–15}. The boundaries of

these basin of attraction are in general fractal^{11,12}. The dynamics within the basin of attraction is governed by the geometry of the stable invariant manifolds associated with the respective equilibrium and the separatrix manifolds of the basin of attraction^{15,16}. Manifolds are the nonlinear extension of the eigenvectors obtained in the linearized dynamics around the equilibrium. Hence, infinitesimal disturbances around the equilibrium are generally exponentially decaying to equilibrium (linear dynamical behavior). However, under certain conditions and unexpectedly, large excursions (larger than the disturbance) can be observed in the basin of attraction. This type of behavior is known as *excitability*. Excitability is a generic phenomenon encountered in many areas of Science and in particular in biology^{17–21}, chemistry^{22,23}, and optics^{24,25}.

From the point of view of the phase portrait geometry, excitability arises because stable invariant manifolds are folded (as a consequence of previous bifurcations) or are connected with hyperbolic points that generate separatrix inside the basin of attraction (see Fig. 1)^{20,21}. Therefore, excitability is a genuine nonlinear phenomenon. The above scenario changes radically when considering excitable systems extending over space. In this context, a local perturbation above the excitability threshold is enough to excite its nearest neighbors, generating excitable pulses or waves^{19,21,26–28}. These waves are known in chemical reactions^{19,27}, in the cardiac muscle¹⁷, and in liquid crystals²⁶. In lasers, their existence has been theoretically predicted in a laser with injected signal²⁸ but the experimental part lack of a convincing demonstration. In most of these works, the propagation of pulses is studied, which has a well-defined propagation speed. However, continuous models are used to characterized the propagation. It is known that discreteness can affect the propagation of waves fronts^{29,30}. For example, the wavefront speed in discrete systems can present oscillations^{29–31}. Even more, discreteness can induce the propagation failure in bistable³² or excitable⁴ discrete systems.

The aims of this manuscript is to study theoretically

^{a)} Electronic mail: sylvain.barbey@c2n.upsaclay.fr

the propagation of pulses in an array of excitable semiconductor lasers. Based on a one-dimensional array of coupled lasers with saturable absorber medium, we show that the propagation of pulses is characterized by a hopping dynamics (see Fig. 1). Depending on the coupling strength between the lasers, we characterize the speed of the pulses and their bifurcation diagrams. This speed increases with the coupling strength. The propagating pulses emerge by means of a saddle-node bifurcation, as the coupling constant increases, then the solution adapts itself and exhibits several instabilities. The observed pulses are peculiar to the discrete nature of the excitable lasers coupling, that is, when the continuous limit is taken, the traveling pulses do not persist.

II. THEORETICAL DESCRIPTION OF AN ARRAY OF EXCITABLE SEMICONDUCTOR LASER

The excitable system that we consider is a micropillar laser with an integrated saturable absorber medium studied theoretically in^{33,34} and experimentally in^{35,36}. These lasers have been shown to behave analogously to biological neurons, displaying refractory periods³⁶, spike latency^{37,38} and temporal summation (coincidence detection)³⁹. We consider a 1D array of evanescently coupled lasers with saturable absorber^{8,10} depicted in Fig. 1a

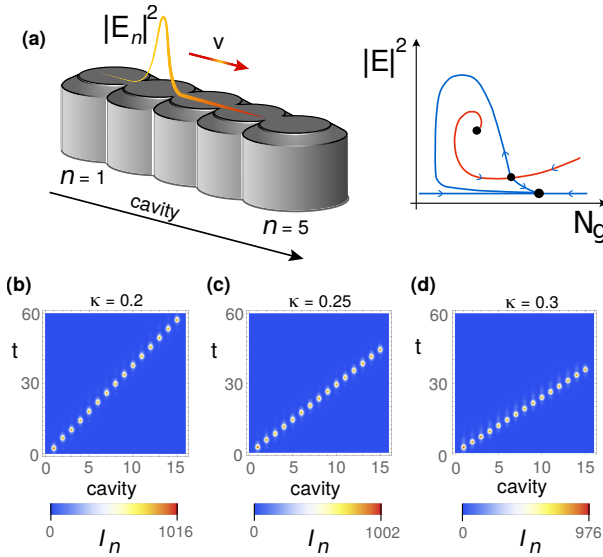


Figure 1. (color online) Pulse propagation in 1D array of excitable semiconductor lasers. (a) Schematic representation of an array of excitable semiconductor lasers. Lasers emit from the top and are evanescently coupled through the neighbors. The inset accounts for the typical phase portrait of a single semiconductor laser. Curves and dots account for invariant manifolds and equilibria. Spatiotemporal propagation of a pulse of an array of excitable semiconductor laser model Eqs. (1)-(3) with different coupling constant $\kappa = 0.20$ (b), $\kappa = 0.25$ (c), and $\kappa = 0.30$ (d), $\alpha = 2.0$, $\beta = 0$, $A = 2.74$, $B = 2$, $b_1 = b_2 = 0.001$, and $s = 10$.

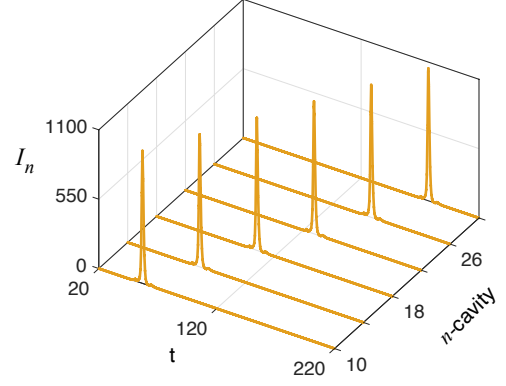


Figure 2. (color online) Pulse propagation in an array of excitable semiconductor laser model Eqs. (1)-(3) with $\alpha = 2.0$, $\beta = 0$, $A = 2.74$, $B = 2$, $b_1 = b_2 = 0.001$, and $s = 10$. Spatiotemporal evolution of a perturbation above excitable threshold of the leftmost cavity, in an array of 100 coupled micropillars with evanescent coupling $\kappa = 0.15$.

and described by the dimensionless set of equations

$$\dot{E}_n = [(1 - i\alpha)N_{g,n} - (1 - i\beta)N_{as,n} - 1] E_n + i\kappa(E_{n-1} + E_{n+1}), \quad (1)$$

$$\dot{N}_{g,n} = b_1 [A - N_{g,n} (1 + |E_n|^2)], \quad (2)$$

$$\dot{N}_{as,n} = b_2 [B - N_{as,n} (1 + s|E_n|^2)], \quad (3)$$

where $E_n(t)$, $N_{g,n}(t)$, and $N_{as,n}(t)$ account respectively for the envelope of the electric field, the rescaled gain and the rescaled absorption in the i -th laser. The factors α and β are standard semiconductor parameters describing phase-amplitude coupling. κ stands for the dispersive nearest-neighbor coupling coefficient between the lasers. Non-radiative carrier recombination rates for the gain and absorber media are, respectively, b_1 and b_2 . A and B account for the pump gain and non-saturable losses. The saturation parameter s in semiconductors is necessarily greater than 1. Time is rescaled to the cavity photon lifetime, which is the shortest timescale in the system (several picoseconds), and the carrier recombination timescales which are of the order of $0.5 - 1$ nanosecond are therefore small: $b_{1,2} \ll 1$. Notice that a model similar to the set of equations (1-3) with purely diffusive coupling has been considered to study synchronization phenomena in the presence of additive noise⁴⁰ and localization phenomena when coefficients are variable (with disorder)⁴¹. The set of equations (1-3) under the influence of noise exhibits synchronization, and with variable coefficients shows localization⁴². A single semiconductor laser with an integrated saturable absorber medium can be accurately described by rate equations for the intensity of the electric field, gain, and absorption, the *Yamada model*^{34,43}. However, because of the evanescent coupling between the microlasers, one must consider the envelope of the electric field in the model written in Eqs. (1-3) to account for the dispersive (imaginary) coupling term.

The non-lasing solution is represented by $E_n(t) = 0$,

$N_{g,n} = A$, and $N_{as,n} = B$. This state is stable for a single laser when $A - B - 1 < 0$ and corresponds to an attractor. Excitable dynamical behavior requires that³³ $s > 1 + 1/B$. Note that in semiconductor materials, this condition is fulfilled since the parameter s is a large parameter due to the gain saturation. The schematic projection of the phase portrait of a single laser in the plane $\{N_g, I = |E|^2\}$ is illustrated in Fig. 1a. The laser threshold corresponds to a transcritical bifurcation and occurs at $A_{th} \equiv 1 + B$. In this kind of system, excitability exists near a homoclinic loop bifurcation and below the laser threshold. If the system is sent above the stable manifold of the saddle point, it makes a large excursion around the heteroclinic orbit and turns back to the stable state corresponding to the off solution of the laser: an excitable optical pulse is produced.

In Figure 1 b-d, pulse propagation in the array of semiconductor lasers is exemplified for different values of the evanescent coupling parameter, κ . This parameter can be experimentally tuned by changing the center-to-center distance between the pillars (see Ref. 44). In the regime of weak evanescent coupling, $\kappa \ll 1$, the coupling time is large as compared to the photon cavity lifetime which ensures that an excitable response can form before the energy couples to the neighboring laser. This corresponds to a saltatory propagation regime¹⁰. When κ is larger, as will be shown below, the propagation mode deviates from the saltatory one. To test numerically the pulse propagation, we disturb a single laser with a perturbation amplitude value slightly above the excitable threshold (cf. Fig. 2). The first effect observed due to the discreteness of the excitable medium is that the propagation of the pulses proceeds through a hopping (or saltatory) dynamics. Namely, the lasers are turned on one by one while they emit an excitable spike, and when they go back to their off state they excite the neighboring lasers. If the coupling strength is large enough, the leaking of energy from the initially perturbed laser to the neighboring ones can excite the neighbors and propagate the pulse. The process repeats giving rise to the observed hopping dynamics. Note that the propagation is unidirectional because of the refractory period exhibited by each excitable laser^{36,37}: once the laser has fired a spike, it cannot be re-excited immediately thus there is a symmetry breaking of the excitable medium. This explains why the pulse that starts at one edge only propagates to a single flank.

III. PULSE SPEED AND BIFURCATION DIAGRAM CHARACTERIZATION

As we increase the value of the evanescent coupling parameter κ , the average pulse speed $\langle v \rangle$ increases. Figure 3 summarizes how the average pulse speed behaves as a function of κ . For small evanescent coupling values, we do not observe propagating pulses. The pulses appear by means of a saddle-node bifurcation from a critical cou-

pling constant $\kappa \equiv \kappa_{sn}$. The saddle-node bifurcation is a generic mechanism of emergence of localized structures in several contexts such as nonlinear optics, plasma, and fluid^{45–49}. The main features of this bifurcation are that solutions are only observed in a region of the parameter space and that a critical exponent is observed near the bifurcation for the growth rate as a function of the distance to the equilibrium. Figure 4 shows the intensity of the electric field in two successive lasers as a function of time for different evanescent coupling regions (I to IV) highlighted on Figure 3. The pulse throughout region I is characterized by the fact that the intensity of the electric field is concentrated in a single laser (see Fig. 4a). Numerically, we find for the parameters considered in figure 2 and close to the left edge (asymptotic limit of the speed) that the mean speed goes almost linearly with κ such that $\langle v \rangle = v_0 + v_1(\kappa - \kappa_{sn})^n$ with $v_0 = 0.06176$, $v_1 = 1.655$, $\kappa_{sn} = 0.1$ and $n = 0.9189$ (cf. Fig. 5a). This regime corresponds to a solitary, ballistic regime.

However, close to $\kappa \equiv \kappa_t = 0.45$ (region II), we observe that there is a qualitative change in the average speed curve (see Fig. 3). Figure 5b shows a zoom of regions I and II. We note that the speed of the pulse varies continuously but is not differentiable at this critical point. To reveal the origin of this instability, the evolution of the electric field intensity in two successive lasers below and above the transition is shown in region II on Fig. 4b,c. Note that below the bifurcation, the temporal profile of the pulse in the two successive lasers is identical. However, above the bifurcation, the temporal profiles in two successive lasers are not identical and they alternate. Therefore, this bifurcation corresponds to a spontaneous translational symmetry-breaking. This

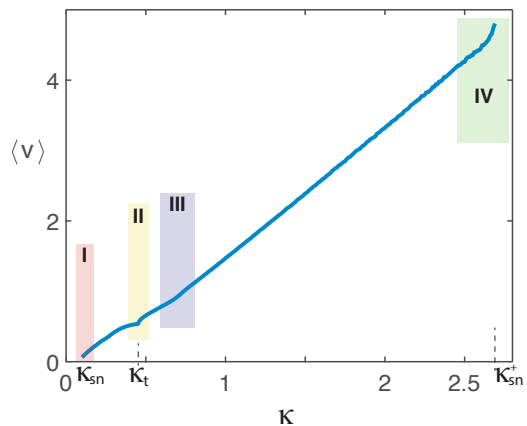


Figure 3. (color online) Average pulse speed as a function of evanescent coupling κ of excitable semiconductor laser model Eqs. (1)-(3) with $\alpha = 2.0$, $\beta = 0$, $A = 2.74$, $B = 2$, $b_1 = b_2 = 0.001$, and $s = 10$. The colored regions account for the different bifurcations observed. $\kappa_{sn} \sim 0.1$, $\kappa_t \sim 0.45$, and $\kappa_{sn}^+ \sim 2.71$ account for the critical evanescent coupling in which the pulses emerge and present a spontaneous symmetry translation-breaking, respectively.

transition occurs for both pulses that propagate to the right or left flank, then one expects this bifurcation to be of the pitchfork type^{11–15}. To characterize the pitchfork bifurcation we fit on Figure 5b the average speed with $\langle v \rangle = a_0 + a_1(\kappa - \kappa_t)^n$ with $a_0 = 0.5363$, $a_1 = 0.6659$, $\kappa_t = 0.454$, and $n = 0.5367$. The dependance is thus compatible with the expected square root law.

Likewise, to characterize the spontaneous translational symmetry-breaking bifurcation, we introduce the total intensity in the n th-laser as an order parameter

$$I_{T,n} = \int dt |E_n|^2(t). \quad (4)$$

Figure 6 shows the total intensity for two successive lasers as a function of the evanescent coupling parameter. Below the bifurcation, the total intensity between two successive lasers is identical. However, above the bifurcation, the total intensity is dissimilar and there is a concentration of energy in one of the lasers. The pulse intensities in successive lasers become almost identical at $\kappa = 0.65$,

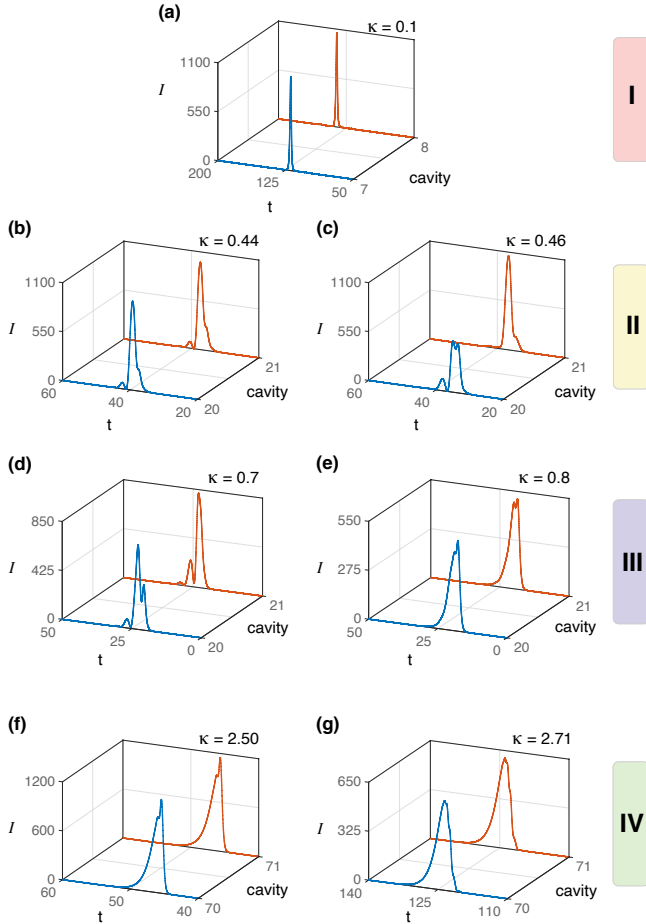


Figure 4. (color online) Intensity of electric field $I = |E_n|^2$ of two successive micropillars as a function of time for different evanescent coupling parameter $\kappa = 0.1$ (a), $\kappa = 0.44$ (b), $\kappa = 0.46$ (c), $\kappa = 0.7$ (d), $\kappa = 0.8$ (e), $\kappa = 2.5$ (f), and $\kappa = 2.71$ (g). Pulses spread to the right flank.

otherwise there is a translational symmetry breaking for $0.44 < \kappa < 0.80$. From $\kappa = 0.80$ onward, the system recovers the spatial translation invariance (cf. Fig. 6). Increasing the value of the coupling κ , the propagative pulses persist for rather large values until they disappear by a saddle-node bifurcation for $\kappa \equiv \kappa_{sn}^+ = 2.71$. For κ greater than κ_{sn}^+ no pulses are observed (see Fig. 3). Physically, this is expected since the energy will flow to the neighboring cavities before reaching the excitable threshold. Therefore, propagation is not possible anymore.

It is worthy to note that the continuous limit of the set of equations (1)-(3) is obtained considering an infinitely large coupling constant ($\kappa \rightarrow \infty$). Therefore, we conclude from the previous observations that in the continuous limit the model Eqs. (1)-(3) has no propagating pulses. In order to support this conjecture, we

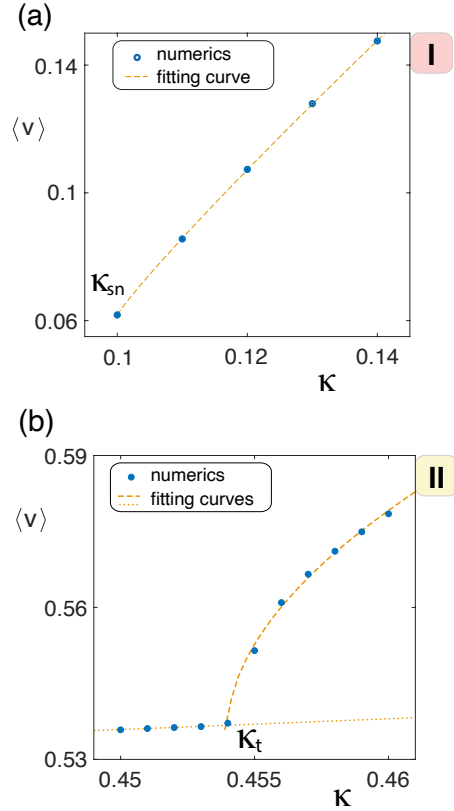


Figure 5. (color online) Amplifications of average pulse speed as a function of evanescent coupling κ of excitable semiconductor laser model Eqs. (1)-(3) with $\alpha = 2.0$, $\beta = 0$, $A = 2.74$, $B = 2$, $b_1 = b_2 = 0.001$, and $s = 10$. Points account for the pulse speed obtained numerically. (a) Emergence of hopping pulse solutions. The dashed curve is obtained by fitting $\langle v \rangle$ with $\langle v \rangle = v_0 + v_1(\kappa - \kappa_{sn})^n$ and $v_0 = 0.06176$, $v_1 = 1.655$, $\kappa_{sn} = 0.1$ and $n = 0.9189$. (b) Spontaneous translational symmetry-breaking instability. The dashed curve is obtained by fitting $\langle v \rangle$ with $\langle v \rangle = a_0 + a_1(\kappa - \kappa_t)^n$ and $a_0 = 0.5363$, $a_1 = 0.6659$, $\kappa_t = 0.454$, and $n = 0.5367$.

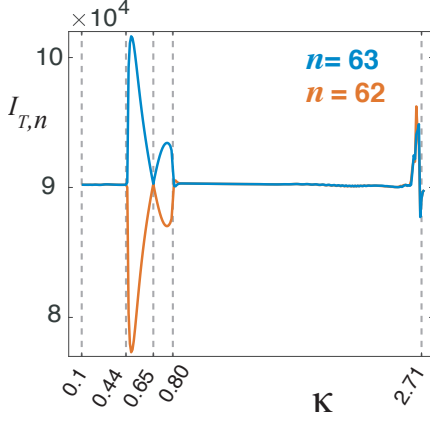


Figure 6. (color online) Total intensity of electric field $I_{T,n}$ in the n -micropillar as a function of evanescent coupling for model Eqs. (1)-(3) with $\alpha = 2.0$, $\beta = 0$, $A = 2.74$, $B = 2$, $b_1 = b_2 = 0.001$, and $s = 10$.

analyze in the parameter space (κ, A) the region where the pulses with hopping dynamics are observed. The results are shown on Figure 7. As the gain pump parameter A decreases, the window of coupling constants where propagating pulses are observed shrinks. Below $A = 2$, no propagating pulses are observed since the system is not excitable anymore. Similar bifurcation diagrams are observed for the average pulse speed for different evanescent coupling constant and pump gain as shown on Figure 7b. Interestingly, the mean speed can also be controlled through the pump⁸ as can be seen on Figure 7c. This is a very important feature from an experimental point of view since the coupling constant is often fixed by fabrication. The yellow shadowed region shows the region where the propagating pulses are observed. Note that for a finite pump gain in the excitable region ($2 < A < 3$) and in the continuous limit, no propagating pulses are expected. The continuous limit of the set of Eqs. (1)-(3) plus diffusive coupling was studied in Refs.^{50,51}. Propagation of pulses is shown for non-radiative carrier recombination rates of the same order as the one of the electric field ($b_1 \sim b_2 \sim 1$). For semiconductor micropillar lasers, these rates differ from several orders of magnitude since the electric field decay time is much smaller than the carrier decay times. Hence, for the typical parameters of micropillar lasers, it is not possible to observe pulses in the continuous limit.

IV. CONCLUSION

Continuous spatially extended excitable systems can sustain the propagation of pulses. This phenomenon is intuitively based on the fact that the system without spatial coupling is excitable, that is, if an equilibrium suffers a sufficiently large disturbance, the dynamical system exhibits large excursions in the basin of attraction.

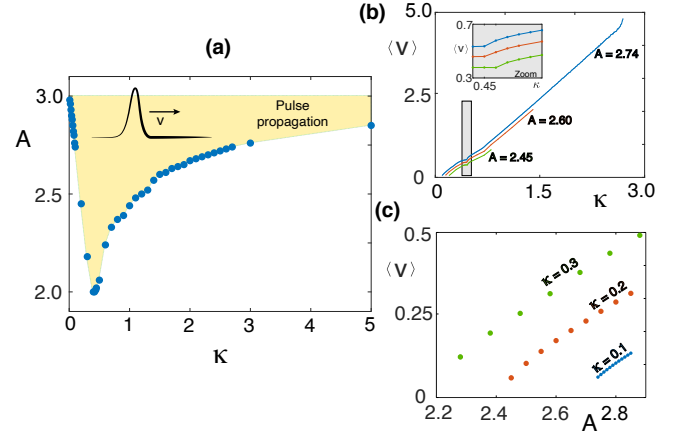


Figure 7. (color online) Phase diagram of pulse obtained for model Eqs. (1)-(3) with $\alpha = 2.0$, $\beta = 0$, $B = 2$, $b_1 = b_2 = 0.001$, and $s = 10$. (a) Pulse phase diagram in A - κ space. Points account for the limits of pulse obtained numerically. Average pulse speed as a function of evanescent coupling κ (b) and pump gain A (c).

When considering the spatially extended system, one expects that when a region is perturbed, it will excite the surrounding areas generating the emission of pulses or waves. The persistence of this phenomenon for coupled (discrete) excitable systems is expected. However, the phenomenon of pulse propagation in discrete, coupled excitable systems is not obvious and depends on the coupling. We show that pulse propagation in discrete, coupled excitable lasers is characterized by a hopping dynamics and that it presents a rich bifurcation structure. We also show that the observed pulses do not necessarily persist in the continuous limit. These results pave the way to the experimental study of such hopping dynamics in optics with potential impact on neuromimetic systems and information processing⁸.

ACKNOWLEDGMENTS

M.G.C. and K.A.B. acknowledge support from Fondo Nacional de Desarrollo Científico y Tecnológico (FONDECYT Project No 1180903) and from Millennium Institute for Research in Optics. S.B. and K.A.B. acknowledge partial support from CNRS.

DATA AVAILABILITY

The data that support the findings of this study are available from the corresponding author upon reasonable request.

REFERENCES

- ¹R. Fitzhugh, *Biophys. J.* **2**, 11 (1962).
- ²J. P. Keener, *SIAM J. Appl. Math.* **47**, 556 (1987).
- ³A. Scott, *Neuroscience* (Springer New York, 2002).
- ⁴A. Carpio and I. Peral, *J. Nonlinear. Sci.* **21**, 499 (2011).
- ⁵H. Waxman, *Scholarpedia* **7**, 1451 (2012).
- ⁶P. R. Prucnal, B. J. Shastri, and M. C. Teich, *Neuromorphic Photonics*, edited by P. R. Prucnal and B. J. Shastri (CRC Press, 2017).
- ⁷J. Feldmann, N. Youngblood, C. D. Wright, H. Bhaskaran, and W. H. P. Pernice, *Nature* **569**, 208 (2019).
- ⁸V. A. Pammi, K. Alfaro-Bittner, M. G. Clerc, and S. Barbay, *IEEE J. Select. Topics Quantum Electron.* **26**, 1 (2020).
- ⁹J. Robertson, M. Hejda, J. Bueno, and A. Hurtado, *Sci. Rep.* **10** (2020), 10.1038/s41598-020-62945-5.
- ¹⁰S. Barbay, I. Sagnes, R. Kuszelewicz, and A. M. Yacomotti, in *2011 Fifth Rio De La Plata Workshop on Laser Dynamics and Nonlinear Photonics* (IEEE, 2011).
- ¹¹E. A. Jackson, *Perspectives of nonlinear dynamics*, Vol. 1 (Cambridge University Press, New-York, 1989).
- ¹²F. C. Hoppensteadt, *Analysis and simulation of chaotic systems* (Springer Verlag, New-York, 2000).
- ¹³S. H. Strogatz, *Nonlinear Dynamics and Chaos* (CRC Press, 2015).
- ¹⁴D. Acheson, *From Calculus to Chaos: An Introduction to Dynamics* (Oxford University Press, 1997).
- ¹⁵J. Guckenheimer and P. Holmes, *Nonlinear Oscillations, Dynamical Systems, and Bifurcations of Vector Fields* (Springer New York, 1983).
- ¹⁶S. Wiggins, *Chaotic Transport in Dynamical Systems* (Springer New York, 1992).
- ¹⁷W. Adelman, *Biophysics and Physiology of Excitable Membranes* (Van Nostrand, 1971).
- ¹⁸D. R. Clothier and J. Brindley, *J. Math. Biol.* **39**, 377 (1999).
- ¹⁹J. D. Murray, *Mathematical Biology* (Springer New York, 2002).
- ²⁰E. M. Izhikevich, *Int. J. Bifurcation Chaos* **10**, 1171 (2000).
- ²¹E. Izhikevich, *Dynamical Systems In Neuroscience* (MIT Press, 2007).
- ²²P. Ruoff, *Chem. Phys. Lett.* **90**, 76 (1982).
- ²³D. Sazou, A. Karantonis, and M. Pagitsas, *Int. J. Bifurcation Chaos* **03**, 981 (1993).
- ²⁴F. Plaza, M. G. Velarde, F. T. Arecchi, S. Boccaletti, M. Ciofini, and R. Meucci, *Europhys. Lett.* **38**, 85 (1997).
- ²⁵M. Giudici, C. Green, G. Giacomelli, U. Nespolo, and J. R. Tredicce, *Phys. Rev. E* **55**, 6414 (1997).
- ²⁶P. Coullet, T. Frisch, J. M. Gilli, and S. Rica, *Chaos* **4**, 485 (1994).
- ²⁷S. Grill, V. S. Zykov, and S. C. Mller, *J. Phys. Chem.* **100**, 19082 (1996).
- ²⁸P. Coullet, D. Daboussy, and J. R. Tredicce, *Phys. Rev. E* **58**, 5347 (1998).
- ²⁹Y. Ishimori and T. Munakata, *J. Phys. Soc. Jpn.* **51**, 3367 (1982).
- ³⁰M. Peyrard and M. D. Kruskal, *Physica D* **14**, 88 (1984).
- ³¹M. G. Clerc, R. G. Elías, and R. G. Rojas, *Philos. Trans. Royal Soc. A* **369**, 412 (2011).
- ³²G. Fáth, *Physica D* **116**, 176 (1998).
- ³³J. L. A. Dubbeldam, B. Krauskopf, and D. Lenstra, *Phys. Rev. E* **60**, 6580 (1999).
- ³⁴J. L. A. Dubbeldam and B. Krauskopf, *Opt. Commun.* **159**, 325 (1999).
- ³⁵S. Barbay, R. Kuszelewicz, and A. M. Yacomotti, *Opt. Lett.* **36**, 4476 (2011).
- ³⁶F. Selmi, R. Braive, G. Beaudoin, I. Sagnes, R. Kuszelewicz, and S. Barbay, *Phys. Rev. Lett.* **112**, 183902 (2014), & Synposis in Physics, *Semiconductors Laser Get Nervy*.
- ³⁷F. Selmi, R. Braive, G. Beaudoin, I. Sagnes, R. Kuszelewicz, T. Erneux, and S. Barbay, *Phys. Rev. E* **94**, 042219 (2016).
- ³⁸T. Erneux and S. Barbay, *Phys. Rev. E* **97** (2018), 10.1103/physreve.97.062214.
- ³⁹F. Selmi, R. Braive, G. Beaudoin, I. Sagnes, R. Kuszelewicz, and S. Barbay, *Opt. Lett.* **40**, 5690 (2015).
- ⁴⁰A. M. Perego and M. Lamperti, *Phys. Rev. A* **94**, 033839 (2016).
- ⁴¹M. Lamperti and A. M. Perego, *Phys. Rev. A* **96**, 041803 (2017).
- ⁴²M. Lamperti and A. M. Perego, *The European Physical Journal B* **92**, 117 (2019).
- ⁴³M. Yamada, *IEEE J. Quantum Electron.* **29**, 1330 (1993).
- ⁴⁴F. Selmi, *Excitable response and neuronlike properties in micropillar lasers with saturable absorber*, *Theses*, Université Paris Sud - Paris XI (2015).
- ⁴⁵O. Descalzi, M. Argentina, and E. Tirapegui, *Phys. Rev. E* **67** (2003), 10.1103/physreve.67.015601.
- ⁴⁶A. P. Misra, K. R. Chowdhury, and A. R. Chowdhury, *Phys. Plasmas* **14**, 012110 (2007).
- ⁴⁷H. Sakaguchi and B. A. Malomed, *Phys. Rev. E* **77** (2008), 10.1103/physreve.77.056606.
- ⁴⁸M. G. Clerc, S. Coulibaly, N. Mujica, R. Navarro, and T. Sauma, *Philos. Trans. Royal Soc. A* **367**, 3213 (2009).
- ⁴⁹F. del Campo, F. Haudin, R. G. Rojas, U. Bortolozzo, M. G. Clerc, and S. Residori, *Phys. Rev. E* **86** (2012), 10.1103/physreve.86.036201.
- ⁵⁰N. N. Rosanov, *Spatial hysteresis and optical patterns* (Springer Science & Business Media, 2002).
- ⁵¹S. V. Fedorov, A. G. Vladimirov, G. V. Khodova, and N. N. Rosanov, *Phys. Rev. E* **61**, 5814 (2000).